AIP Advances

Stress induced enhanced polarization in multilayer BiFeO3/BaTiO3 structure with improved energy storage properties

Savita Sharma, Monika Tomar, Ashok Kumar, Nitin K. Puri, and Vinay Gupta

Citation: AIP Advances **5**, 107216 (2015); doi: 10.1063/1.4934578
View online: http://dx.doi.org/10.1063/1.4934578
View Table of Contents: http://scitation.aip.org/content/aip/journal/adva/5/10?ver=pdfcov
Published by the AIP Publishing

Stress induced enhanced polarization in multilayer $BiFeO_3/BaTiO_3$ structure with improved energy storage properties

Savita Sharma,[1,3] Monika Tomar,[2] Ashok Kumar,[4] Nitin K. Puri,[3] and Vinay Gupta[1,a]
[1]*Department of Physics and Astrophysics, University of Delhi, Delhi, India*
[2]*Physics Department, Miranda House, University of Delhi, Delhi, India*
[3]*Department of Applied Physics, Delhi Technological University, Delhi, India*
[4]*CSIR-National Physical Laboratory, Dr. K.S .Krishnan Marg, Delhi, India*

(Received 28 August 2015; accepted 12 October 2015; published online 20 October 2015)

Present work reports the fabrication of a multilayer (5-layer) structure of $BiFeO_3$(BFO)/$BaTiO_3$(BTO) using spin-coating technique. The crystallographic structure, surface morphology and ferroelectric behavior of multilayer structure in metal-ferroelectric-metal capacitor have been studied. Le-Bail refinement of X-ray diffraction data revealed the formation of polycrystalline pure perovskite phase with induced stress. The values of remnant (P_r) and saturation polarization (P_s) for BFO/BTO multilayer structure are found to be 38.14 $\mu C/cm^2$ and 71.54 $\mu C/cm^2$ respectively, which are much higher than the corresponding values reported for bare BFO thin film. A large value of dielectric constant of 187 has been obtained for multilayer structure with a low leakage current density of 1.09×10^{-7} A/cm^2 at applied bias of 10 V. The BFO/BTO multilayer structure favors the enhanced energy storage capacity as compared to bare BFO thin film with improved values of energy-density and charge-discharge efficiency as 121 mJ/cm^3 and 59% respectively, suggesting futuristic energy storage applications. [http://dx.doi.org/10.1063/1.4934578]

INTRODUCTION

The atomic scale combination of dissimilar materials is expected to produce not only striking control but also ample scope of enhancement in new combinations of functional properties. In recent years, novel multilayers comprising of different ferroelectric/multiferroic materials have been intensively studied to find better system with superior electrical and ferroelectric properties having strong coupling and interaction among its layers.[1–4] The interfacial strain due to the lattice mismatch can lead to modulation of ferromagnetic anisotropy and improvement in electrical properties. Also, the ferroelectric switching affects the interface magnetization due to the change in collection of spin-polarized electrons at the ferromagnetic/ferroelectric (FM/FE) interface, as was discussed by many workers for $Fe/BaTiO_3$,[5] $Co_2MnSi/BaTiO_3$[6] and $Fe_3O_4/BaTiO_3$[7] hetrostructures. Reddy *et al*. reported improved ferroelectric as well as ferromagnetic properties for four-layered thin films over two-layered BLFCO-BFO thin films due to the interface coupling and interaction between the thin layers.[8] Pintilie *et al*. studied the capacitance of PZO–PZT (80/20) multilayers with enhanced polarization with increase in number of interfaces due to the presence of some interfacial polarization, trapped charges at the multilayer interfaces.[9] Lee *et al*. studied the enhancement of polarization by strain in superlattices of $BaTiO_3$, $SrTiO_3$ and $CaTiO_3$.[10] Wu *et al*. observed the high saturation polarization in a $(BaTiO_3)_8/(SrTiO_3)_3$ superlattice film.[11] Bao discussed that constructing multilayers or superlattices is an effective way to improve properties of ferroelectric/dielectric thin films.[12]

[a]Email: vgupta@physics.du.ac.in, drguptavinay@gmail.com

Such systems can be effectively combined for the high density ferroelectric random access memory (FE-RAM) and energy storage devices.

Due to the marked improvement in integration of modern electric system, there are great needs for systems which can harness energy from natural sources i.e. implicit self-powered energy storage devices for "green" energy capable of producing both high power and high energy density which can replace batteries to power the microelectronic devices like health monitoring systems, wireless sensors, mobile communication systems etc.[13,14] Two important aspects of energy storage devices are high energy density i.e. capability of storing energy per unit volume or mass and high power density i.e. capability of discharging the stored energy quickly to the external load. Our area of interest focuses on these two aspects although it is difficult to obtain both at the same time.[13] Besides this, low dielectric loss and economic cost are the other important factors to pay attention to. The $BaTiO_3$, $PbTiO_3$ and $CaCuTiO_3$ with large dielectric permittivity are generally employed in energy storage applications, however, due to their low electrical breakdown strength, these ceramic materials exhibit poor energy storage properties.[15]

Among various multiferroic materials, BFO has captivated most of the researchers owing to the existence of two ferroic orders simultaneously at room temperature with a Curie temperature (T_C) of 1103 K and Neel temperature (T_N) of 643 K which enables it to be used for high temperature applications.[16–19] However, the device applications of BFO are mainly hindered due to the high leakage current resulting in poor ferroelectric properties.[16] These problems can also be overcome by combining two or more ferroelectric materials with multiferroic materials retaining the excellent room temperature ferromagnetism in BFO. The resultant structure may yield superior properties compared to the individual constituent materials enabling it to be used for device applications. Recent studies on BFO have confirmed the existence of large magnetization and ferroelectric polarization in strained thin films. Few workers reported improvement in the electric and magnetic properties, as well as a large magnetoelectric coupling in the hetrostructure of BFO such as $La_{0.7}Sr_{0.3}MnO_3$ (LSMO)/BFO, Fe_2O_4/BFO, CoFe/BFO, Co/BFO, Ni/BFO and $BiTiO_3$/BFO, due to the interface coupling interaction between the individual layers.[20–22] The BTO is a potential ferroelectric material which has been used widely from the last many decades in device applications.[23–25] On the contrary, BTO does not possess ferromagnetic properties. Hence, combining the two ferroic materials i.e. BTO and BFO might give rise to better multiferroic properties.[26–28] Some research groups have studied BFO/BTO multilayered structures, but their strain induced polarization and energy storage properties are scarcely reported.[29] Touplet *et al*. and Yang *et al*.[30,31] reported an improvement in the magnetic property of the BFO/BTO multilayered system due to the interfacial effects and the multiferroic coupling between them.

Film deposition process are also known to affect the properties of deposited thin films or layered structures. Sol-gel spin coating method is known to be the simplest and cost effective for the deposition of BTO and BFO thin films while maintaining appropriate stoichiometry. Hence, in the present work, an effort has been made to prepare a multilayered (five-layer) structure of BFO/BTO on Pt/Ti/SiO_2/Si substrate using sol-gel spin coating method with the improved electrical property.

EXPERIMENTAL

The multilayered structure of BFO/BTO is deposited on platinized silicon (Pt/Ti/SiO_2/Si) substrates using sol-gel spin coating technique. Prior to the deposition of BFO/BTO multilayer structure, the thin film of Pt (70 nm thickness) was deposited over the passivated Si (SiO_2/Si) substrate by E-beam evaporation technique. A buffer layer of Ti (20 nm) was deposited *in-situ* over SiO_2/Si substrate prior to Pt deposition to improve its adhesion. The precursors for the synthesis of BTO and BFO were barium acetate ($Ba(CH_3COO)_2$), bismuth nitrate ($(Bi(NO_3)_3.5H_2O$), iron nitrate ($(Fe(NO_3)_3.9H_2O$), titanium n-butoxide ($Ti(C_4H_9O)_4$). Acetic acid and 2-methoxyethanol were used as solvents and acetylacetone was used as the chelating agent. The BTO thin film was deposited on Pt coated Si substrate as a first layer by spin coating technique and was annealed at 800°C for one hour. It was followed by the deposition of BFO thin film as second layer with annealing at 550°C for two hours to get BFO/BTO structure. Similar process was repeated to get five layered structure namely BTO/BFO/BTO/BFO/BTO on Pt/Ti/SiO_2/Si substrate with total thickness

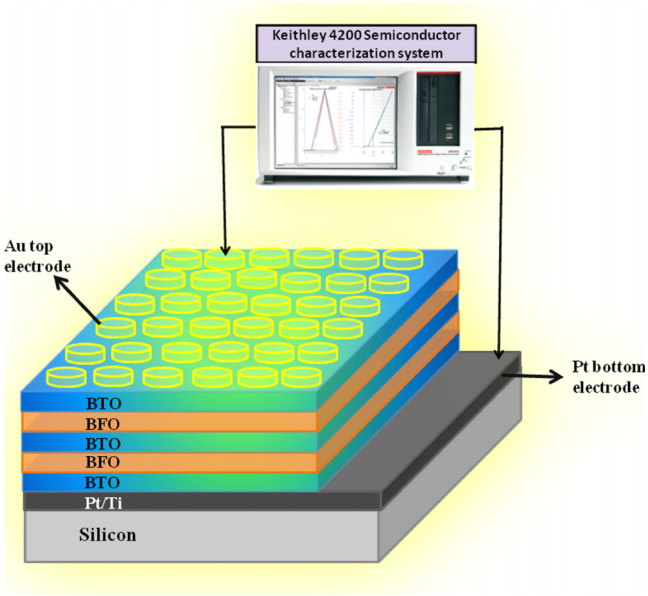

FIG. 1. Schematic of the MFM capacitor configuration of the BFO/BTO multilayer structure deposited on Pt/Ti/SiO_2/Si substrate with Au top electrodes.

of 350 nm, the average thickness of each layer being ~70 nm. For electrical measurements, circular top electrodes of Au metal (200 μm diameter, 40 nm thickness) were deposited on the BFO/BTO surface by thermal evaporation technique through a shadow mask. The schematic of prepared metal-ferroelectric-metal (MFM) capacitor configuration (Au/BTO/BFO/BTO/BFO/BTO/Pt/SiO_2/Si) is shown in figure 1.

X-ray diffraction (XRD) technique (Bruker D8) was used to study the crystalline structure of the BFO/BTO bilayer structure. The surface morphology of multilayer structure was studied using scanning electron microscopy (SEM) (FEI Quanta 200 F). A Radiant Technology precision ferroelectric workstation was used to measure the room temperature ferroelectric polarization-electric field (P-E) hysteresis loop of the prepared multilayer sample in MFM capacitor configuration at a frequency of 1 kHz and applied bias of 10 V. The current-voltage (I-V) and capacitance-voltage (C-V) characteristics of prepared sample were studied using a semiconductor characterization system (Keithley; 4200 SCS) at room temperature.

RESULTS AND DISCUSSION

Figure 2(a) shows the XRD pattern of the prepared multilayer (BFO/BTO) structure on Pt/Ti/SiO_2/Si substrate. The diffraction peaks corresponding to constituent BFO and BTO were obtained which confirm the growth of multilayer structure of BTO and BFO films of polycrystalline nature. However, no peak exhibiting the formation of any secondary phase in the prepared multilayer structure was obtained. The polycrystalline nature of deposited rhombohedral distorted structure of BFO and tetragonal structure of BTO is clearly evident from Fig. 2(b). Lattice parameters "a" and "c" and c/a distortion ratio for both BTO and BFO layers in BFO/BTO multilayer structure were determined using the Le-Bail intensity extraction method with the help of commercially available Bruker TOPAS 3 Software. The estimated values of lattice parameters (a, c), the volume of unit cell and the strain induced along 'c' axis for both BFO and BTO thin films in the multilayer structure are summarized in Table I. The corresponding reported values for bulk BFO and BTO are also included in Table I for comparison. The value of lattice parameters, a and c are estimated to be 4.256 Å and 4.079 Å, respectively, for BTO thin film and 5.518 Å and 13.561 Å, respectively, for BFO thin film. The obtained values of lattice parameters for BFO thin film are slightly lower than the corresponding bulk values for BFO but for BTO thin film, the values are greater than that of bulk

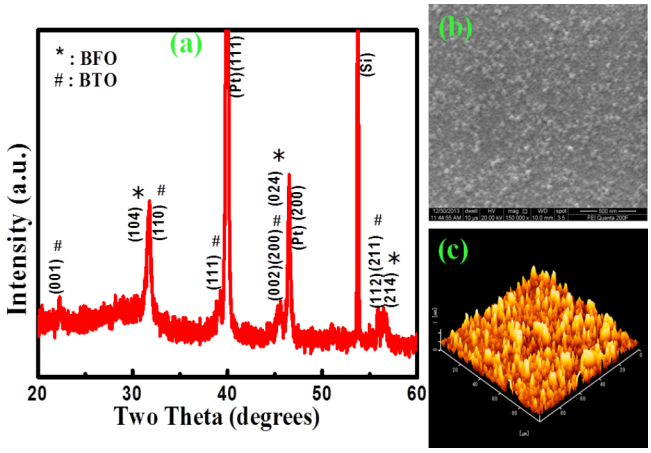

FIG. 2. (a) XRD pattern of BFO/BTO multilayer structure deposited on platinized silicon substrate, (b) SEM image of BFO/BTO multilayer structure (c) A 100 μm X 100 μm AFM image of the surface of BFO/BTO multilayer structure.

BTO [JCPDS card No. 01-072-0138 and 01-072-2035]. The results obtained indicate the presence of tensile stress and compressive stress in the BFO and BTO thin films in multilayer structure. The value of stress modulus (%) for BTO and BFO thin films is found to be about 1.1405% and 2.206%, respectively. The large value of stress modulus in BFO thin film is responsible for the increase in the lattice distortion which leads to an improvement in ferroelectric property of the multilayer structure. Fig. 2(b) shows the SEM micrograph of the surface of BFO/BTO multilayer structure. It can be clearly seen from Fig 2(b) that the prepared multilayer structure has a dense and smooth surface with uniformly distributed grains of ~40 nm size. The AFM image of the surface of prepared BFO/BTO multilayer structure is shown in Fig. 2(c). The homogeneous distribution of grains of ~40 nm size is seen on the surface of BFO thin film (Fig. 2(c)), which is in agreement with the SEM micrograph. The root mean square (RMS) value of the roughness (R_a) of the surface of multilayer structure lies between 10 and 15 nm (Fig. 2(c)).

Fig. 3 shows the semi-log plot of current versus voltage (I-V) for the multilayer structure of BFO/BTO and bare BFO thin film recorded with both polarities of the applied voltage at room temperature. Both the I-V curves exhibit good symmetry under both applied positive and negative bias in terms of the absence of any barrier at the electrode and the presence of ohmic contacts. However, a significant difference in the leakage current density for multilayer is observed in comparison to that of bare BFO film. Leakage current (1.09×10^{-7} A) of multilayer BFO/BTO structure was found to be two order less in comparison to that of bare BFO thin film (1.10×10^{-5} A) with an applied voltage of 10 V. The obtained results show significant reduction in the leakage current density with fabrication of artificial multilayer. The presence of ferroelectric BTO layer helps in reducing the leakage current by two orders of magnitude which is desirable for functional device applications. The reduced leakage current in multilayer structure is due to the blocking of ions migration by resistive ferroelectric BTO layers and the presence of trap centers of carriers formed

TABLE I. Lattice parameters "a" and "c", c/a distortion ratio and stress modulus along c-axis for the BTO and BFO thin films in BFO/BTO multilayer structure.

	BTO thin film				**BFO thin film**			
	Lattice parameter		**Stress**	**c/a distortion**	**Lattice parameter**		**Stress**	**c/a distortion**
	a (Å)	**c (Å)**	**Modulus (%)**	**ratio**	**a (Å)**	**c (Å)**	**Modulus (%)**	**ratio**
Bulk	3.999	4.033	—	1.0085	5.876	13.867	—	2.3599
Multilayer	4.256	4.079	1.1405	0.9584	5.518	13.561	2.206	2.4575

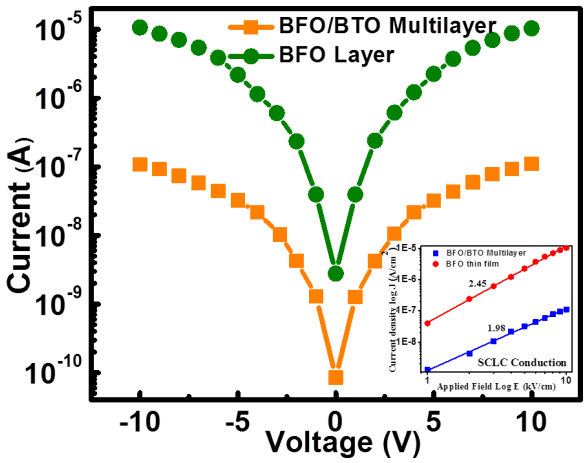

FIG. 3. I-V characteristics of BFO/BTO multilayer structure and bare BFO thin film. Inset shows the variation in leakage current density as a function of electric field fitted with SCLC mechanism.

at the interfaces between BFO and BTO films. Also, the surface roughness might result in the decrease of the leakage current. Jo *et al*. and Xu *et al*. reported the superior electrical and ferroelectric properties in the case of PZT/BFO and $BaSrTi_{1.1}O_3/BaSrTi_{1.05}O_3/BaSrTiO_3$ multilayer thin films, respectively.[32,33] It may be recalled that the bare BFO thin film has a high leakage current when grown on the Pt-coated Si substrate. Further, BFO/BTO multilayer system exhibits a stable insulating behaviour over the entire measured range of applied voltage. Inset of figure 4 represents the log–log plot of J–E which exhibits linear behaviour over the entire voltage range for pure BFO thin film as well as BFO/BTO multilayer structure. The slope of the straight line is found to be 2.45 and 1.98, respectively, confirming trap assisted SCLC behavior. Hence, it may be inferred that the leakage current in BFO and BFO/BTO multilayer thin films exhibits trap-controlled SCLC transport at applied electric fields.

Figure 4 shows the capacitance-voltage (C-V) characteristics for the BFO/BTO multilayer system in MFM capacitor configuration. Inset (a) of Fig. 5 shows the dielectric vs. voltage curve measured for BFO/BTO multilayer system while inset (b) shows the capacitance-voltage (C-V) characteristics of bare BFO thin film for the comparison. The observed characteristic butterfly loop (Fig. 5) confirms the good ferroelectric property of the prepared BFO/BTO multilayer structure.

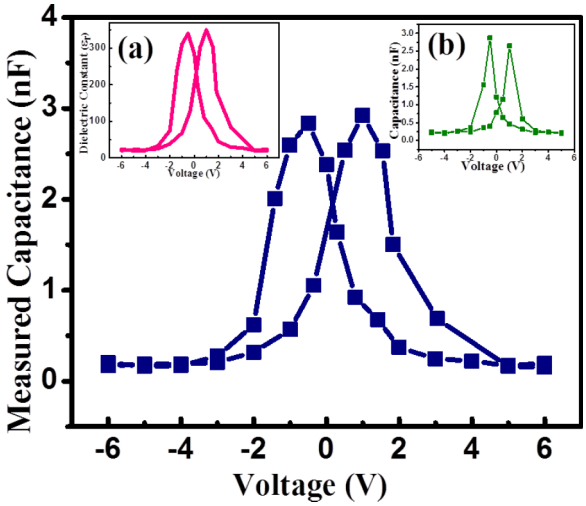

FIG. 4. C-V characteristics of BFO/BTO multilayer structure. Inset (a) shows the dielectric vs. voltage curve measured for BFO/BTO multilayer system while inset (b) shows the capacitance-voltage (C-V) characteristics of bare BFO thin film for the comparison.

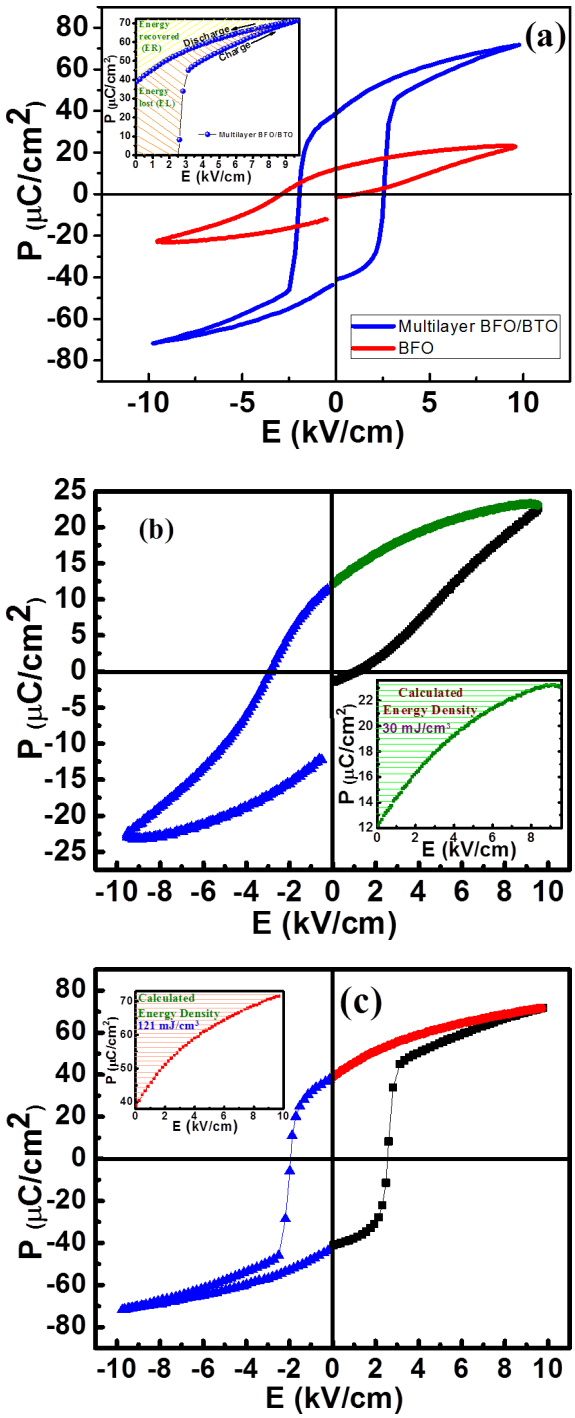

FIG. 5. (a) Room temperature ferroelectric (P-E) hysteresis curves of BFO/BTO multilayer structure and bare BFO thin film. Inset of (a) Yellow Shaded area of P–E loop illustrates the capacity to store (recoverable) energy and orange shaded area the energy loss. (b) and (c): Room temperature ferroelectric P-E hysteresis loop of the BFO thin film and BFO/BTO multilayer structure respectively, along with inset representing the stored energy density (shaded area shown) corresponding to PE loops.

The two peaks at applied bias of +1 V and -0.6 V in the C-V curve (Fig. 5) reveal the polarization reversal of the ferroelectric domains in the multilayer system. Further it can be seen from Fig 5 that the capacitance tends to a constant value C_o with increase in the magnitude of applied bias. The capacitance can be written as $C_o = \varepsilon_o.\varepsilon_r.S/d$, where ε_o is the permittivity of vaccum

TABLE II. Ferroelectric properties, Leakage current and Energy density of BFO/BTO multilayer structure and single layered BFO thin film.

	$P_r(\mu C/cm^2)$	$P_s(\mu C/cm^2)$	$2E_c$ (kV/cm)	Leakage current (A)	U_{ER} (mJ/cm^3)	U_{EL} (mJ/cm^3)	U_{ET} (mJ/cm^3)	η(%)
BFO	12.52	23.24	4.08	1.10 x 10^{-5}	30	105	135	22
Multilayer BFO/BTO	38.14	71.54	4.53	1.09 x 10^{-7}	121	84	205	59

(8.85 x 10^{-12} F/m); ε_r is the relative dielectric constant of BFO/BTO multilayer; S is the electrode area (3.14 x 10^{-8} m^2) and d is the thickness of the multilayer system (350 nm). Considering the value of C_o as 0.15 nF at ±6 V (Fig. 5), the estimated value of ε_r for BFO/BTO multilayer system is about 187, which is higher than the corresponding reported value of the dielectric constant for bare BTO or BFO thin film.[34,35] The obtained results clearly highlight the importance of combining BTO and BFO thin films. The combination of both layers enhances the coupling between the ferroelectric and ferromagnetic domains that lead to a net high polarization for the BFO/BTO multilayer structure.

Figure 5(a) shows the room temperature ferroelectric (P-E) hysteresis curves of BFO/BTO multilayer structure and bare BFO thin film at 1 KHz over an applied bias range from -10 V to +10 V. The yellow shaded area in the inset of fig. 5(a) illustrates the energy storage capacity (recoverable energy), whereas the orange shaded portion reflects the energy loss. It may be seen from Fig. 5(a) that the ferroelectric property of the multilayer structure is enhanced in comparison to the bare BFO thin film. The obtained values of remnant polarization (P_r), saturation polarization (P_s) and coercive field (E_c) for the multilayer structure along with that of bare BFO thin film are summarized in Table II. The BFO/BTO multilayer system exhibits the maximum saturation polarization (P_s) of about 71.54 μC/cm^2 and remnant polarization (P_r) of 38.14 μC/cm^2 (Fig. 5(a)). The enhanced ferroelectric property of the BFO/BTO multilayer structure may be related to the induced strain at the interface of two layers and large lattice distortion (c/a ratio).

Energy storage capacity of BFO/BTO multilayer system is estimated from the P-E hysteresis loop.[36] Fig. 5(b) and 5(c) shows the room temperature ferroelectric P-E hysteresis loop of BFO and BFO/BTO multilayer structure, respectively. The shaded area shown in the inset corresponds to the stored energy density (recoverable energy). The green shaded area in the inset of Fig. 5(b) represents the energy density recovered (ER) and the red shaded area inside the loop in the inset of Fig. 5(c) represents the energy loss (EL). The sum of ER and EL represents the total energy density (ET) stored in the material. The charge–discharge efficiency η can then be calculated by $\eta = (U_{ER}/U_{ET}) \times 100\%$.[15] All the calculated values of energy density and efficiency for BFO/BTO multilayer structure and bare BFO thin film have been tabulated in Table II. To minimize the size and weight of capacitors, thin films with high recoverable energy density (U_{ER}) and high charge-discharge efficiency (η) are required. The U_{ER} value for BFO thin film structure was found to be ~30 mJ/cm^3 with an energy loss of 105 mJ/cm^3, while for BFO/BTO multilayer structure, the enhanced U_{ER} value of 121 mJ/cm^3 was obtained with reduced energy loss of 84 mJ/cm^3 (Table II). The η value of BFO thin film was 22% while it is greatly enhanced in the case of BFO/BTO multilayer structure to 59% (Table II). This enhancement in U_{ER} and η values and the reduction in energy loss observed for BFO/BTO multilayer structure favors its potential usage in energy storage applications.

CONCLUSION

The BFO/BTO multilayer structure was fabricated on Pt/Ti/SiO_2/Si substrate by sol-gel spin coating technique. X-ray diffraction studies reveal the formation of polycrystalline and pure phase of perovskite structure for both BTO and BFO. Electrical study of the multilayer structure indicates an enhancement in ferroelectric properties (P_s = 71.54 μC/cm^2 and P_r = 38.14 μC/cm^2) and reduction in leakage current by two orders (1.09 x 10^{-7} A) in comparison to that of bare BFO

film. The improved electrical properties of the multilayer system is related to the coupling between the ferroelectric and ferromagnetic domains of BTO and BFO, respectively, that lead to an enhancement in polarization in the multilayer structure. Low leakage current (0.1 μA) and improved energy density (121 mJ/cm^3) with high charge-discharge efficiency (59%) obtained for BFO/BTO multilayer structure suggests its futuristic energy storage applications.

ACKNOWLEDGEMENT

Authors are thankful to Department of Science and Technology (DST), University of Delhi and Delhi Technological University (DTU) for providing all the facilities to carry out the research work.

[1] R. Nechache, P. Gupta, C. Harnagea, and A. Pignolet, Appl. Phys. Lett. **91**, 222908 (2007).
[2] N. Ichikawa, M. Arai, Y. Imai, K. Hagiwara, H. Sakama, M. Azuma, Y. Shimakawa, M. Takano, Y. Kotaka, M. Yonetani, H. Fujisawa, M. Shimizu, K. Ishikawa, and Y. Cho, Appl. Phys. Exp. **1**, 101302 (2008).
[3] H. C. Ding, Y. W. Li, W. Zhu, Y. C. Gao, S. J. Gong, and C. G. Duan, J. Appl. Phys. **113**, 123703 (2013).
[4] M. Dawber, N. Stucki, C. Lichtensteiger, S. Gariglio, P. Ghosez, and J. M. Triscone, Adv. Mater. **19**, 4153–4159 (2007).
[5] S. Valencia, A. Crassous, L. Bocher, V. Garcia, X. Moya, R. O. Cherifi, C. Deranlot, K. Bouzehouane, S. Fusil, A. Zobelli, A. Gloter, N. D. Mathur, A. Gaupp, R. Abrudan, F. Radu, and A. Barthélémy, Nature Materials **10**, 753 DOI: 10.1038/nmat3098 (2011).
[6] L. Y. Chen, C. L. Chen, K. X. Jin, and X. J. Du, EPL **99**, 57008 DOI: 10.1209/0295-5075/99/57008 (2012).
[7] T. L. Qu, Y. G. Zhao, P. Yu, H. C. Zhao, S. Zhang, and L. F. Yang, Appl. Phys. Lett. **100**, 242410 DOI: 10.1063/1.4729408 (2012).
[8] V. A. Reddy, N. Dabra, K. K. Ashish, J. S. Hundal, N. P. Pathak, and R. Nath, Adv. Mater. Lett. **6**(8), 678–683 (2015).
[9] L. Pintilie, K. Boldyreva, M. Alexe, and D. Hesse, New Journal of Physics **10**, 013003 (2008).
[10] H. N. Lee, H. M. Christen, M. F. Chisholm, C. M. Rouleau, and D. H. Lowndes, Nature **433**, 27 (2005).
[11] P. Wu, X. Ma, Y. Li, V. Gopalan, and L. Q. Chen, Appl. Phys. Lett. **100**, 092905 (2012).
[12] D. Bao, Current opinion in solid state and material science **12**, 55–61 (2008).
[13] C. A. Paz de Araujo, J. D. Cuchiaro, L. D. Mcmillan, M. C. Scott, and J. F. Scott, Nature **374**, 627 (1994).
[14] S. A. Sherrill, P. Banerjee, G. W. Rubloff, and S. B. Lee, Phys. Chem. Chem. Phys. **13**, 20714 (2011).
[15] Z. Hu, B. Ma, S. Liu, M. Narayanan, and U. Balachandran, Ceram. Int. **40**, 557–562 (2014).
[16] J. F. Ihlefeld, N. J. Podraza, Z. K. Liu, R. C. Rai, X. Xu, T. Heeg, Y. B. Chen, J. Li, R. W. Collins, J. L. Musfeldt, X. Q. Pan, J. Schubert, R. Ramesh, and D. G. Schlom, Appl. Phys. Lett. **92**, 142908 (2008).
[17] S. Gupta, M. Tomar, and V. Gupta, J. Exp. Nanosci. **8**(3), 261 (2013).
[18] H.W. Chang, F.T. Yuan, Y.C. Yu, P.C. Chen, C.R. Wang, C.S. Tu, and S.U. Jen, J. Alloys Compd. **574**, 402 (2013).
[19] K. Jiang, J. J. Zhu, J. D. Wu, J. Sun, Z. G. Hu, and J. H. Chu, Appl. Mater. Interf. **3**, 4844 (2011).
[20] Q. Xu, Z. Wen, J. Gao, D. Wu, S. Tang, and M. Xu, Physica B **406**, 2025 DOI : 0.1016/j.physb.2011.03.011 (2011).
[21] H. Singh, A. Kumar, and K. L. Yadav, Mat. Sci. Eng. B **176**, 540 DOI: 10.1016/j.mseb.2011.01.010 (2011).
[22] V. A. Reddy, N. Dabra, J. S. Hundal, N. P. Pathak, and R. Nath, Science of Advanced Materials **6**, 1043 (2014).
[23] I. Kingon, J. P. Maria, and S. K. Streiffer, Nature **406**, 1032 (2000).
[24] K. J. Choi, M. Biegalski, Y. L. Li, A. Sharan, J. Schubert, R. Uecker, P. Rerche, Y. B. Chen, X. Q. Pan, V. Gopalan, L. Q. Chen, D. G. Schlom, and C. B. Eom, Science **306**, 1005 (2004).
[25] V. Vaithyanathan, J. Lettieri, W. Tian, A. Sharan, A. Vasudevarao, Y. L. Li, A. Kochhar, H. Ma, J. Levy, P. Zschack, J. C. Woicik, L. Q. Chen, V. Gopalan, and D. G. Schlom, J. Appl. Phys. **106**, 024108 (2009).
[26] S. Sharma, M. Tomar, A. Kumar, N. K. Puri, and V. Gupta, Physica B **448**, 125–127 (2014).
[27] S. Sharma, M. Tomar, A. Kumar, N. K. Puri, and V. Gupta, Adv. Sci. Lett. **20**, 1316–1320 (2014).
[28] M. Kumar, A. Srinivas, and S.V. Suryanarayana, J. Appl. Phys. **87**(2), 855 (2000).
[29] M. Lorenz, V. Lazenka, P. Schwinkendorf, F. Bern, M. Ziese, H. Modarresi, A. Volodin, M. J. V. Bael, K. Temst, A. Vantomme, and M. Grundmann, J. Phys. D: Appl. Phys **47**, 135303 (2014).
[30] H. Toupet, V. V. Shvartsman, F. Lemarrec, P. Borisov, W. Kleemann, and M. Karkut, Integ. Ferroelectrics **100**, 165–176 (2008).
[31] P. Yang, K. M. Kim, J. Y. Lee, J. Zhu, and H. Y. Lee, Integrated Ferroelectrics **113**, 26–30 (2009).
[32] Z. Xu, D. Yan, D. Xiao, P. Yu, and J. Zhu, Ceramics International **39**, 1639–1643 (2013).
[33] S. H. Jo, S. G. Lee, and S. H. Lee, Materials Research Bulletin **47**, 409–412 (2012).
[34] D. Huang, H. Deng, P. Yang, and Junhao Chu, Mater. Lett. **64**, 2233–2235 (2010).
[35] R. R. Das, Y. I. Yuzyuk, P. Bhattacharya, V. Gupta, and R. S. Katiyar, Phys. Rev. B **69**, 132302 (2004).
[36] H. Borkar, V. N. Singh, B. P. Singh, M. Tomar, V. Gupta, and A. Kumar, RSC Adv. **4**, 22840 (2014).